Chemosphere 194 (2018) 360–369

Contents lists available at ScienceDirect

Chemosphere

journal homepage: www.elsevier.com/locate/chemosphere

Immobilization of hexavalent chromium in contaminated soils using biochar supported nanoscale iron sulfide composite

Honghong Lyu [a, d], Hang Zhao [a], Jingchun Tang [a, *], Yanyan Gong [b, **], Yao Huang [a], Qihang Wu [c], Bin Gao [d]

[a] Key Laboratory of Pollution Processes and Environmental Criteria (Ministry of Education), Tianjin Engineering Center of Environmental Diagnosis and Contamination Remediation, College of Environmental Science and Engineering, Nankai University, Tianjin 300350, China
[b] School of Environment, Guangzhou Key Laboratory of Environmental Exposure and Health, and Guangdong Key Laboratory of Environmental Pollution and Health, Jinan University, Guangzhou 510632, China
[c] Collaborative Innovation Center of Water Quality Safety and Protection in Pearl River Delta, Guangzhou University, Guangzhou 510006, China
[d] Department of Agricultural and Biological Engineering, University of Florida, Gainesville, FL 32611, United States

HIGHLIGHTS

- First study on CMC-FeS@biochar for enhanced Cr(VI) immobilization in soil.
- Surface sorption and reduction/precipitation are dominant immobilization mechanisms.
- The composite converts more accessible Cr into less accessible forms.
- The composite greatly reduces bioavailability of Cr(VI) to wheat and earthworms.
- The addition of the composite enhances soil organic matter and microbial activity.

GRAPHICAL ABSTRACT

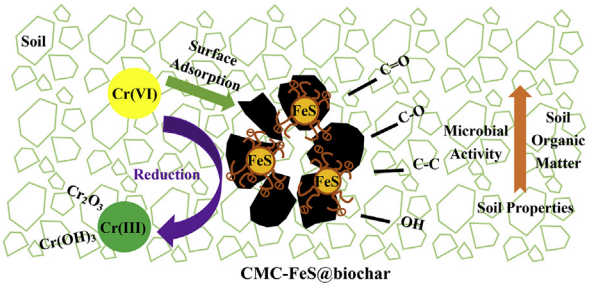

ARTICLE INFO

Article history:
Received 11 September 2017
Received in revised form
14 November 2017
Accepted 30 November 2017
Available online 1 December 2017

Handling Editor: Patryk Oleszczuk

Keywords:
Iron sulfide
Biochar
Cr(VI) immobilization
Reduced toxicity
Soil remediation

ABSTRACT

Biochar supported carboxymethyl cellulose (CMC)-stabilized nanoscale iron sulfide (FeS) composite (CMC-FeS@biochar) was prepared and tested for immobilization of hexavalent chromium Cr(VI) in soil. Results of UV–vis and transmission electron microscopy (TEM) showed that the backbone of biochar suppressed the aggregation of FeS, resulting in smaller particle size and more sorption sites than bare FeS. The composite at a dosage of 2.5 mg per gram soil displayed an enhanced Cr(VI) immobilization efficiency (a 94.7% reduction in the toxicity characteristic leaching procedure (TCLP) based leachability and a 95.6% reduction in the $CaCl_2$ extraction) compared to plain biochar and bare FeS. Sequential extraction procedure (SEP) and X-ray photoelectron spectroscopy (XPS) analysis suggested that CMC-FeS@biochar promoted the conversion of more accessible Cr (exchangeable and carbonate-bound fractions) into the less accessible forms (iron-manganese oxides-bound, organic material-bound, and residual fractions) to reduce the toxicity of Cr(VI) and that surface sorption and reduction were dominant mechanisms for Cr(VI) immobilization. CMC-FeS@biochar greatly reduced the bioavailability of Cr(VI) to wheat and earthworms (*Eisenia fetida*). Moreover, the application of CMC-FeS@biochar enhanced soil organic matter content and microbial activity. This work highlighted the potential of CMC-FeS@biochar

* Corresponding author.
** Corresponding author.
E-mail addresses: tangjch@nankai.edu.cn (J. Tang), yanyangong@jnu.edu.cn (Y. Gong).

https://doi.org/10.1016/j.chemosphere.2017.11.182

composite as a low-cost, “green”, and effective amendment for immobilizing Cr(VI) in contaminated soils and improving soil properties.

1. Introduction

Chromium (Cr) is widely used in a variety of industrial applications, such as electroplating, metallurgy, leather tanning, wood preservation, and chromate manufacturing. The acidic industrial wastewater containing high content of Cr can lead to a widespread contamination of the surrounding soil (Ajmal et al., 1984; Koenig et al., 2016). A nationwide survey of soil pollution conducted in 2014 in China showed that chromium contents of the soil sampling points exceeded the standard rate by 1.1% (Faisal and Hasnain, 2005). Cr(VI) and Cr(III) are the two oxidation states of Cr in natural environment. Cr(III) is less toxic, easy to hydrolyze in aqueous solution ($Cr(OH)_3$, Cr_2O_3), and recognized as an essential trace element for human nutrition, while Cr(VI) is hyper-toxic and soluble in aqueous media over a wide pH range. Due to its carcinogenicity, persistence, and bioaccumulation, Cr contamination causes the accumulation of Cr in plants, enters the food chain via plants, and eventually presents potential threat to human health (Husson, 2013). Sivakumar and Subbhuraam (EPD and MLR, 2014) reported that Cr(VI) was lethal to earthworms at concentrations ranging from 225 to 257 mg kg^{-1} in soil. In China, chromium is regulated with a critical value of 1000 mg kg^{-1} for total Cr (Cr_{total}) and 30 mg kg^{-1} for Cr(VI) in soil of commercial use. Thus, it is important to reduce the potential toxicity of Cr(VI) in soil by converting Cr(VI) to insoluble Cr(III) precipitates, which can be immobilized in soil.

In situ remediation of Cr(VI)-contaminated soil by delivering reactive materials into input source zones has recently been considered as a promising technology (Fang et al., 2016; Mahdieh et al., 2016; Su et al., 2016). Su et al. (2016) reported that nano zero-valent iron@biochar (nZVI@biochar) composite reduced the toxicity characteristic leaching procedure (TCLP)-leachable Cr(VI) concentrations from Cr(VI) spiked soil (Cr(VI) content = 320 mg kg^{-1}) by 100% and decreased the physiological based extraction test (PBET)-based bioaccessibility of Cr(VI) by 100% when the soil was treated with 8 g kg^{-1} of nZVI@biochar for 15 d. Pot experiments showed that nZVI@biochar effectively reduced Cr contents in the leaves, stems, and roots of the cabbage mustard by 78.8%, 86.9%, and 83.4%, respectively. However, when applied to environmental remediation, ZVI may preferentially reduce nitrate and/or oxygen which may not be the targets, leading to a decrease in the immobilization efficiency (Henderson and Demond, 2011).

Iron sulfide (FeS) is effective for the reduction of Cr(VI) because it can provide a source of Fe(II) and S (-II) species. However, bare FeS particles tend to agglomerate rapidly, greatly diminishing their removal efficiency. The introduction of carboxymethyl cellulose (CMC) as a stabilizer and biochar as a Supporting Material can effectively prevent the aggregation of particles and enhance their physical stability and removal efficiency (Gong et al., 2014; Yan et al., 2014). Our previous work indicated that biochar supported nanoscale FeS (CMC-FeS@biochar) was effective in the removal of aqueous Cr(VI) (Lyu et al., 2017). The composite offered higher removal capacity and affinity toward Cr(VI) compared to bare FeS and plain biochar due to a synergistic effect induced by interaction between individual components. The Cr(VI) removal capacity (q_m = 150 mg g^{-1}) was much greater than the reported value of biochar-supported ZVI (10.6 mg g^{-1}). Moreover, the synthetic procedure of CMC-FeS@biochar is simple and environmentally friendly, and no costly chemicals are required. Yet, the feasibility of CMC-FeS@biochar for remediating Cr(VI)-contaminated soil has not been reported.

Biochar related materials are among the most commonly used adsorbents for the immobilization of heavy metals in soils due to their relatively high sorption capacities and friendly environmental compatibility. Cao et al. (2011) reported that biochar could decrease the leaching of Pb(II) in soils and reduce their uptake by earthworms. Significant increases in seed germination and growth have been reported in the soils amended with biochars (Zhou et al., 2013; Ahmad et al., 2014; Sun et al., 2014). However, the biological effects of the CMC-FeS@biochar composite to earthworms and plants are still unclear. Information about the fate and eco-toxicity of Cr species in CMC-FeS@biochar-remediated soil is urgently needed before field application.

The overall goal of this study was to determine the feasibility of CMC-FeS@biochar for immobilization of Cr(VI) in Cr-contaminated soils. The specific objectives were to (1) examine the effects of CMC-FeS@biochar dosage and equilibrium time on the effectiveness of Cr(VI) immobilization; (2) examine the change of Cr speciation in treated soil and explore the underlying Cr(VI) immobilization mechanisms; (3) evaluate the ecological uptake of Cr in earthworms in remediated soil; and (4) determine the effects of CMC-FeS@biochar on seeds germination, early growth, and the bioaccumulation of Cr.

2. Materials and methods

2.1. Materials

All chemicals used in the present study were of analytical grade. Sodium sulfide nonahydrate ($Na_2S·9H_2O$), iron sulfate heptahydrate ($FeSO_4·7H_2O$), and potassium dichromate ($K_2Cr_2O_7$) were purchased from Fengchuan Chemical Technology (Tianjin, China). CMC (in the sodium form, M.W. = 90 000, degree of substitute = 0.7, melting point = 274 °C, and density = 1.6 g cm^{-3}) were purchased from Anpel Laboratory Technology (Shanghai, China). Wheat (Shannong26) seeds were purchased from Zaozhuang Seed Company (Shandong, China). Earthworms (*Eisenia fetida*) were purchased from Jurong Wang Jun earthworm breeding base (Jiangsu, China). Wheat straw obtained from Shandong province, China was air-dried for 7 d and milled into powders of 2 mm as the feedstock biomass for biochar production.

2.2. Soil sample preparation and analysis

A Cr(VI)-free soil sample was obtained from Nankai University in Tianjin, China. Before use, the soil was washed three times with tap water to remove suspended colloids and water leachable compositions. The washed soil was then air-dried for 7 d, and sieved through a standard sieve of 2-mm opening. Cr_{total} content was determined per the US Environmental Protection Agency (EPA) method 3050B (1996) and Cr(VI) content was determined per the US EPA method 3050A (1996). The Cr_{total} content was 31.1 ± 2.9 mg kg^{-1} and no detectable Cr(VI) was found. To prepare

Cr(VI)-contaminated soil, 10 L of 300 mg L^{-1} $K_2Cr_2O_7$ solution was mixed with 10 kg of pretreated soil and stirred until the mixture was air-dried. The final Cr_{total} and Cr(VI) contents in the soil were 320 ± 24 and 210 ± 18 mg kg^{-1}, respectively (Table 1), which were 6 times higher than the discharge limit of 30 mg kg^{-1} for Cr(VI) in soil of commercial use (EPD and MLR, 2014).

Soil pH was measured on a 1:1 soil: water mixture following the Agricultural Standard of China (NY/T 1377–2007). Total organic carbon (TOC) was determined by TOC analyzer (Multi N/C 3100, Analytik Jena, Jena, Germany) with a detection limit of 0.004 g kg^{-1}. Soil redox potential was determined via the Soil–Determination of Redox Potential–Potential method (HJ 746–2015). Soil CO_2, CH_4, N_2O, and NH_3 concentrations were measured by Picarro G2508 Greenhouse Gas Analyzer (Picarro Inc., Santa Clara, CA, USA). Surface elemental compositions of the soil before and after immobilization by CMC-FeS@biochar were analyzed by X-ray photoelectron spectroscopy (XPS) (PHI-5000, ULVAC-PHI, Chigasaki, Japan). The soil before CMC-FeS@biochar treatment was collected directly from the air-dried Cr(VI)-contaminated soil. The soil after CMC-FeS@biochar treatment was prepared by mixing 0.98 g CMC-FeS@biochar with 392 g soil (dry weight = 392 g, i.e., 2.5 mg g^{-1}) for 180 d. The solids were air-dried and collected for XPS analysis.

The fractions of various Cr species in soil were analyzed following the sequential extraction procedure (SEP) developed by Tessier et al. (1979), which partitions metals into five fractions, i.e., exchangeable (EX), carbonate (CB)-bound, iron-manganese oxides (OX)-bound, organic material (OM)-bound, and residual (RS) fractions (Tessier et al., 1979). The relative availability follows the order of EX > CB > OX > OM > RS (Su et al., 2016), and OX, OM, and RS are relatively stable fractions. Note that the extractions were analyzed for aqueous Cr_{total}.

2.3. Preparation and characterization of CMC-FeS@biochar composite

CMC-FeS@biochar was prepared following our previously reported approach (Lyu et al., 2017) and the details are provided in the Supporting Information (SI, Section 1). The resultant CMC-FeS@biochar containing 500 mg L^{-1} FeS, 500 mg L^{-1} CMC, and 500 mg L^{-1} biochar (i.e., FeS: CMC: biochar mass ratio = 1:1:1) was used in the subsequent experiments unless indicated otherwise. For comparison, plain biochar and bare FeS were prepared under otherwise identical conditions.

The ultraviolet–visible (UV–vis) absorption spectra of CMC-FeS@biochar were obtained using a UV–visible spectrophotometer (Shimadzu UV-3600, Shimadzu, Kyoto, Japan) in the wavelength range of 200–900 nm. Transmission electron microscopy (TEM) was carried out using a T-20 transmission electron microscope (Philips, Amsterdam, Holland) to investigate the surface structure and morphology of the samples.

2.4. Immobilization of Cr(VI) in soil by CMC-FeS@biochar

Batch experiments were conducted in 500 mL glass beakers containing 400 g of Cr-contaminated soil with the addition of various dosage of CMC-FeS@biochar composite, namely, 2.5, 5.0, and 10 mg g^{-1}. The composite dosage was determined based on the maximum aqueous Cr(VI) removal capacity of CMC-FeS@biochar (SI Table S1) (Lyu et al., 2017), Cr(VI) content in the soil, and our preliminary experimental results. Bare FeS and plain biochar were incubated with soils at a dosage of 2.5 mg g^{-1}, respectively. 90 mL of deionized water was added to keep a moisture content of 20 ± 5%. The beakers were then sealed and stored in the dark at room temperature (25 ± 2 °C). After predetermined time intervals (3, 7, 14, 30, 60, 90, and 180 d), 25 g of soil was collected for soil properties analysis. Control tests were conducted in the absence of CMC-FeS@biochar under otherwise identical conditions. All experiments were conducted in duplicate, and the average values are reported.

To evaluate the effects of CMC-FeS@biochar amendments on Cr mobility, TCLP tests were performed following the Environmental Protection Industry Standard of China (HJ/T300-2007). The detailed procedure is provided in SI, Section 2. To assess the Cr bioavailability to soil organisms, $CaCl_2$ extraction experiments were carried out following a revised method by Cao et al. (2011). 4 g sample was extracted with 40 mL of 0.01 M $CaCl_2$ solution containing 25 mg L^{-1} NaN_3 to minimize microbial activity (Cao et al., 2011). After mixing on an end-over-end rotator at 30 rpm for 24 h, samples were settled by gravity for 30 min and the supernatant was filtered by 0.45-μm mixed cellulose ester membrane filters. The filtrates were analyzed for aqueous Cr(VI), Cr_{total}, and Fe concentrations.

2.5. Effects of CMC-FeS@biochar on Cr uptake by earthworms

Earthworms play a paramount role in soil health and are one of the most commonly used receptors for assessing ecological uptake of contaminants in soils. The uptake of Cr by earthworm (*Eisenia foetida*) was performed following a reported method by Petersen et al. (2009) as described in SI, Section 3 (Petersen et al., 2009). The damage level of the DNA strands in the earthworm cells was determined using a comet assay following a method by Liu et al. (2010b) and Hu et al. (2015). Three earthworms were selected to conduct the electrophoresis and staining experiments. The stained slides were viewed using a fluorescence microscope (Zeiss, Axio Imager Z1, Germany) equipped with a CCD camera. The captured images were analyzed using the CASP software, and the percentage of tail DNA (% DNA) was measured as an indicator of DNA damage (Liu et al., 2010b; Hu et al., 2015).

2.6. Effects of CMC-FeS@biochar on seed germination, early growth, and Cr bioaccumulation

Wheat growth experiments were conducted to investigate the

Table 1
Selected physio-chemical properties of the soils used in this study.

Soil	pH	Total organic carbon (g kg^{-1})	Redox potential (mV)	Cr_{total} (mg kg^{-1})	Cr(VI) (mg kg^{-1})
Cr(VI)-free soil	8.37 ± 0.12	<0.004	518 ± 30	31.1 ± 2.9	<0.16
Cr(VI)-contaminated soil	7.86 ± 0.04	<0.004	374 ± 19	320 ± 24	210 ± 18
2.5 mg g^{-1} biochar + Cr(VI)-contaminated soil	7.95 ± 0.03	19.2 ± 0.6	350 ± 13	308 ± 16	128 ± 14
2.5 mg g^{-1} FeS + Cr(VI)-contaminated soil	7.82 ± 0.04	6.7 ± 1.3	339 ± 15	319 ± 21	69.4 ± 9.8
2.5 mg g^{-1} CMC-FeS@biochar + Cr(VI)-contaminated soil	7.68 ± 0.04	13.1 ± 0.1	320 ± 17	321 ± 14	12.9 ± 1.8
5.0 mg g^{-1} CMC-FeS@biochar + Cr(VI)-contaminated soil	7.58 ± 0.01	19.3 ± 1.7	317 ± 12	305 ± 10	9.0 ± 1.1
10 mg g^{-1} CMC-FeS@biochar + Cr(VI)-contaminated soil	7.53 ± 0.03	22.6 ± 0.9	300 ± 9	316 ± 17	8.2 ± 0.9

effects of CMC-FeS@biochar on the plant growth and the accumulation of Cr(VI). Seed germination tests were conducted by spreading 20 wheat seeds on a flat plate covered with three layers of filter paper. The Cr(VI) content was set at 1.92 mg container^{-1} based on previous reported study about the inhibitory effect of Cr(VI) on pigeon pea seeds (Dotaniya et al., 2014) and our preliminary experiments, and the amount of CMC-FeS@biochar (0.016 g container^{-1}) was calculated accordingly based on the maximum aqueous Cr(VI) removal capacity of CMC-FeS@biochar (SI Table S1) (1.25 times of the calculated value). Control tests were conducted in the absence of CMC-FeS@biochar (containing the same amount of Cr(VI) as the Cr(VI)-laden CMC-FeS@biochar). Blank tests were performed with the addition of 6 mL deionized water into the container. Each treatment was carried out in duplicate, covered, and incubated in the dark at room temperature. Germination percentage was assessed after 2 d. After 12 d growth, all of the wheat plants were harvested, washed thoroughly with deionized water, and the germinal length was measured, subsequently oven dried at 85 °C for 30 min. The Cr_{total} contents in the dried plants were determined using a method by Wang et al. (2014) (SI, Section 4).

2.7. Analytical methods

Cr(VI) concentrations of TCLP leachates, $CaCl_2$ leachates, and soil digestion solution were determined using an UV–vis Spectrophotometer (754, Chuangyuanbo Technology Development, Tianjin, China) following the Environmental Protection Standard of China (GB 7467-87). The detection limit was 0.004 mg L^{-1}. The concentrations of Cr_{total} and Fe were determined by inductively coupled plasma atomic emission spectrometry (ICP-AES) (IRIS Intrepid II XSP, Thermo Elemental, Massachusetts, USA). The method afforded a detection limit of 4.3 and 2.0 μg L^{-1}, respectively. Cr(III) concentrations were calculated according to mass balance.

3. Results and discussion

3.1. Characterization of CMC-FeS@biochar composite

The UV–vis spectra provide a convenient indication of the formation of CMC-FeS@biochar composite (Fig. 1). For individual homogeneous solutions of Fe^{2+}, CMC, S^{2-}, and CMC–Fe^{2+} complexes, no absorbance occurred at 260–800 nm. When biochar was added into the CMC–Fe^{2+} solution, the complex showed a weak absorbance profile over a broad wavelength of 200–900 nm without any distinctive peak. When S^{2-} ions were further introduced, the solution color rapidly turned black, showing strong absorbance peaks at 347 nm and 660 nm. Introduction of S^{2-} led to *in-situ* formation of FeS on the surface of the biochar. In contrast, the suspension of bare FeS did not show any characteristic peak. No conspicuous change in the UV–vis spectra of CMC-FeS@biochar was observed after 24 h, indicating that the composite was stable physically and chemically.

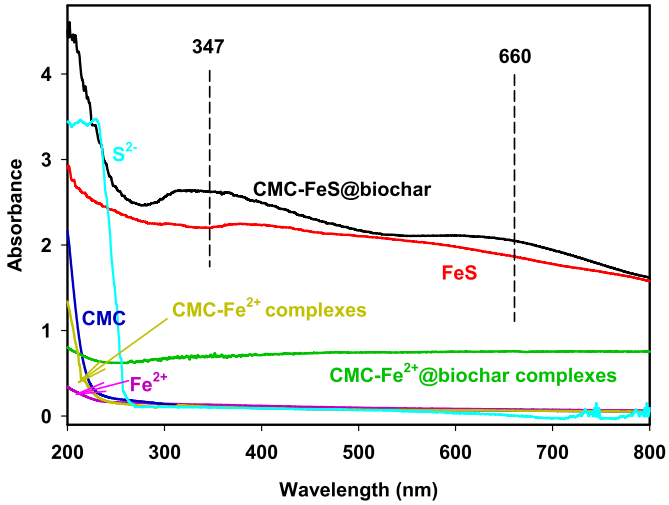

Fig. 1. UV–vis absorption spectra of 31.8 mg L^{-1} Fe^{2+}, 50 mg L^{-1} CMC, CMC-Fe^{2+}complexes (50 mg L^{-1} CMC, 31.8 mg L^{-1} Fe^{2+}), CMC-Fe^{2+}@biochar complexes (50 mg L^{-1} CMC, 31.8 mg L^{-1} Fe^{2+}, 50 mg L^{-1} biochar), 18.2 mg L^{-1} S^{2-}, 50 mg L^{-1} FeS, and CMC-FeS@biochar (50 mg L^{-1} CMC, 31.8 mg L^{-1} Fe^{2+}, 50 mg L^{-1} biochar, 18.2 mg L^{-1} S^{2-}, FeS: CMC: biochar mass ratio = 1:1:1).

TEM images of FeS, biochar, and CMC-FeS@biochar are shown in Fig. 2. FeS particles mainly present as aggregated flocs (Fig. 2A), and the surface of biochar was smooth (Fig. 2B). There were clearly defined and discrete FeS particles located on the CMC-FeS@biochar surface (Fig. 2C and D), resulting in a larger specific surface area (51.5 m^2 g^{-1} for CMC-FeS@biochar vs. 6.4 m^2 g^{-1} for FeS), pore size (16.2 nm for CMC-FeS@biochar vs. 14.3 nm for FeS), pore volume (0.07 cm^3 g^{-1} for CMC-FeS@biochar vs. 0.02 cm^3 g^{-1} for FeS), and thus, more sorption sites.

3.2. Immobilization of Cr(VI)

TCLP has been widely used to evaluate the immobilization of heavy metals in soils to indicate remediation effectiveness. TCLP-leachable Cr(VI) concentrations in untreated and biochar-, FeS-, or CMC-FeS@biochar-treated soils were compared (Fig. 3A). For the untreated soil, the TCLP-leachable Cr(VI) concentration remained constant at 11.9–12.2 mg L^{-1} over 180 d. The immobilization efficiency was enhanced as the treatment time increased from 3 to 60 d (upon equilibrium). For instance, Cr(VI) concentrations in the TCLP leachates reduced significantly from 2.15 mg L^{-1} after 3 d to 0.65 mg L^{-1} after 60 d. For 2.5 mg g^{-1} FeS, Cr(VI) concentrations in TCLP leachates displayed a rapid reduction within 60 d (from 3.47 to 2.96 mg L^{-1}). Upon equilibrium, further increasing the reaction time to 180 d, the TCLP-leachable Cr(VI) remained constant, i.e., 0.63 mg L^{-1} upon 2.5 mg g^{-1} CMC-FeS@biochar treatment, 2.91 mg L^{-1} upon 2.5 mg g^{-1} FeS, and 6.30 mg L^{-1} upon 2.5 mg g^{-1} biochar. After 180 d, CMC-FeS@biochar (2.5 mg g^{-1}) reduced TCLP-leachable Cr(VI) by 94.7% (from 11.9 to 0.63 mg L^{-1}), which was much higher than that of 2.5 mg g^{-1} biochar (from 11.9 to 6.30 mg L^{-1}, a 47.1% decrease) and 2.5 mg g^{-1} FeS (from 11.9 to 2.91 mg L^{-1}, a 75.5% decrease). Increasing the CMC-FeS@biochar dosage from 2.5 to 5.0 and further to 10 mg g^{-1} reduced the TCLP-leachable Cr(VI) concentrations by 94.7%, 96.5%, and 96.6%, respectively. It should be noted that with the application of CMC-FeS@biochar at a dosage of 2.5 mg g^{-1}, the TCLP-leachable Cr(VI) concentrations meet the TCLP threshold of 1.5 mg L^{-1} for Cr(VI) in municipal solid waste (MEPPRC, 2008).

Similar trend was observed for the $CaCl_2$ extraction tests (Fig. 3B). Compared to the untreated soil, $CaCl_2$-extractable Cr(VI) concentrations in CMC-FeS@biochar-treated soils were significantly reduced, and the immobilization efficiency increased with increasing CMC-FeS@biochar dosage (from 2.5 to 10 mg g^{-1}) and treatment time (from 3 to 180 d). After 180 d, CMC-FeS@biochar at 2.5 mg g^{-1} reduced $CaCl_2$-extractable Cr(VI) concentration by 95.6%, compared to 65.5% for 2.5 mg g^{-1} biochar and 91.6% for 2.5 mg g^{-1} FeS. Taken together TCLP- and $CaCl_2$-leachable Cr(VI) concentrations, the optimum dosage of CMC-FeS@biochar was determined to be 2.5 mg g^{-1}.

CMC-FeS@biochar was more effective in immobilizing soil Cr(VI) than bare FeS, which was related to the larger specific surface area (51.5 m^2 g^{-1} for CMC-FeS@biochar vs. 6.4 m^2 g^{-1} for FeS), and

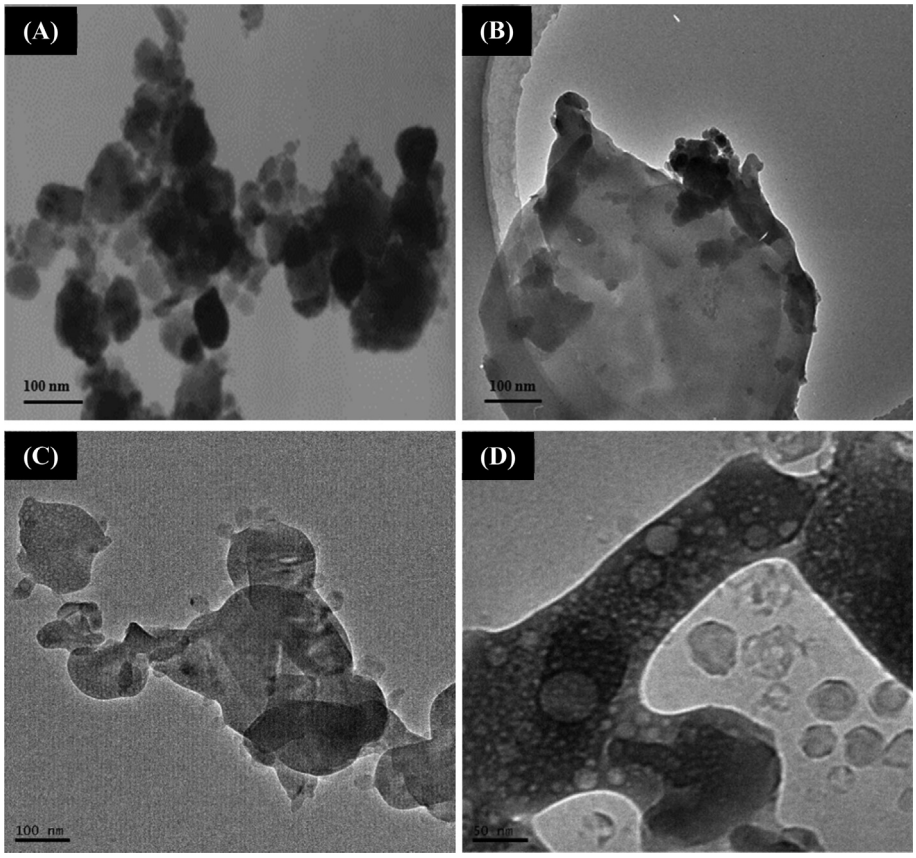

Fig. 2. TEM images of (A) FeS, (B) biochar, (C) CMC-FeS@biochar, and (D) high-magnification image of CMC-FeS@biochar.

thus more sorption sites. CMC-FeS@biochar offered higher Cr(VI) immobilization ability than plain biochar, although biochar had greater specific surface area than CMC-FeS@biochar (51.5 m^2 g^{-1} for CMC-FeS@biochar vs. 215.7 m^2 g^{-1} for biochar), indicating the important role of FeS in Cr(VI) immobilization.

After 180 d, the Cr_{total} and Cr(III) concentrations in the TCLP and $CaCl_2$ extractions were also determined (Fig. 3C and D). Cr_{total} concentrations decreased significantly after the treatment. For instance, upon 2.5 mg g^{-1} CMC-FeS@biochar treatment, Cr_{total} concentrations decreased by 84.8% in TCLP extraction and 88.5% in $CaCl_2$ extraction. As shown in Fig. 3C, TCLP-leachable Cr(III) (7.61 mg L^{-1}) accounted for 39.0% of the Cr_{total} amount (19.5 mg L^{-1}) in the untreated soil. The percentage increased to 78.7% upon 2.5 mg g^{-1} CMC-FeS@biochar treatment, higher than that for 2.5 mg g^{-1} biochar (40.6%) and 2.5 mg g^{-1} FeS treatment (56.7%). The results suggested that the reduction of Cr(VI) to Cr(III) was responsible for Cr(VI) immobilization. In $CaCl_2$ extracts (Fig. 3D), Cr(III) amount (4.89 mg L^{-1}) accounted for 52.1% of the Cr_{total} amount (9.39 mg L^{-1}) in the untreated soil. The addition of 2.5 mg g^{-1} CMC-FeS@biochar increased the Cr(III) percentage by 49.3%, compared to 33.2% for 2.5 mg g^{-1} biochar treatment and 38.7% for 2.5 mg g^{-1} FeS addition, indicating that the CMC-FeS@biochar effectively converted Cr(VI) to Cr(III), therefore, reducing the mobility and bioavailability of Cr(VI) in the soil.

3.3. Cr(VI) immobilization mechanisms by CMC-FeS@biochar

SEP analysis was performed for soils before and after 2.5 mg g^{-1} biochar-, 2.5 mg g^{-1} FeS-, or 2.5 mg g^{-1} CMC-FeS@biochar-treatment to probe the speciation transformation of Cr (Fig. 4). Cr species in the control test (Cr(VI)-contaminated soil) were EX (33.6%), CB (12.9%), OX (40.8%), OM (9.5%), and RS (3.2%). The EX and CB in the 2.5 mg g^{-1} biochar-treated soil decreased to 27.8% and 10.1%, respectively, while OX, OM, and RS increased to 41.4, 14.5, and 6.2%, respectively. The change may be attributed to the sorption of Cr(VI) onto biochar surface through oxygen-containing functional groups (Lyu et al., 2016a). For the 2.5 mg g^{-1} FeS-treated soil, the EX fraction decreased sharply to 1.5%, while OX significantly increased to 62.6%, which was probably due to the formation of Cr_2O_3, $Cr(OH)_3$ and Cr(III)-Fe(III) oxides/hydroxides. Upon 2.5 mg g^{-1} CMC-FeS@biochar treatment, the EX fraction in the soil was completely converted to OX (from 40.8% to 73.1%) and OM (from 9.5% to 11.9%). The CB decreased to 8.1%. CMC-FeS@biochar promoted the conversion of more accessible Cr (EX and CB) into the less accessible forms (OX and OM), thus reduced the toxicity of Cr(VI).

The chemical compositions and oxidation states of the soil before and after 2.5 mg g^{-1} CMC-FeS@biochar treatment were characterized by XPS (Fig. 5). For Cr(VI)-contaminated soil, the C 1s spectra in Fig. 5A exhibited six peaks, namely, C–C at 284.6 eV, C–O at 286.1 eV, C=O at 289.4 eV, and C–F at 292.9, 293.9, and 296.2 eV (Liu et al., 2010a; Wu et al., 2014; Yang et al., 2014). Binding energies of O 1s (Fig. 5B) at 531.8 and 532.2 eV were ascribed to C–O and –OH (Zhou et al., 2007). The Fe 2p3 spectra in Fig. 5C was deconvoluted into two peaks at 712.8 and 725.6 eV, which were assigned to Fe(III) in $Fe(OH)_3$ and/or Fe_2O_3 and Fe(II) (Briggs and Seah, 1993). The peak located at 162.6 eV was ascribed to S (-II), and the peak located at 169.2 and 174.4 eV were ascribed to S(IV) and/or S(VI) (Fig. 5D) (Wagner, 1978). Furthermore, binding energies of Cr 2p3 (Fig. 5E) at 573.9 and 576.8 eV correspond to Cr_2O_3 and/or $Cr(OH)_3$, and binding energy at 582.1 eV was characteristic of Cr(VI) (Choppala et al., 2012, 2015).

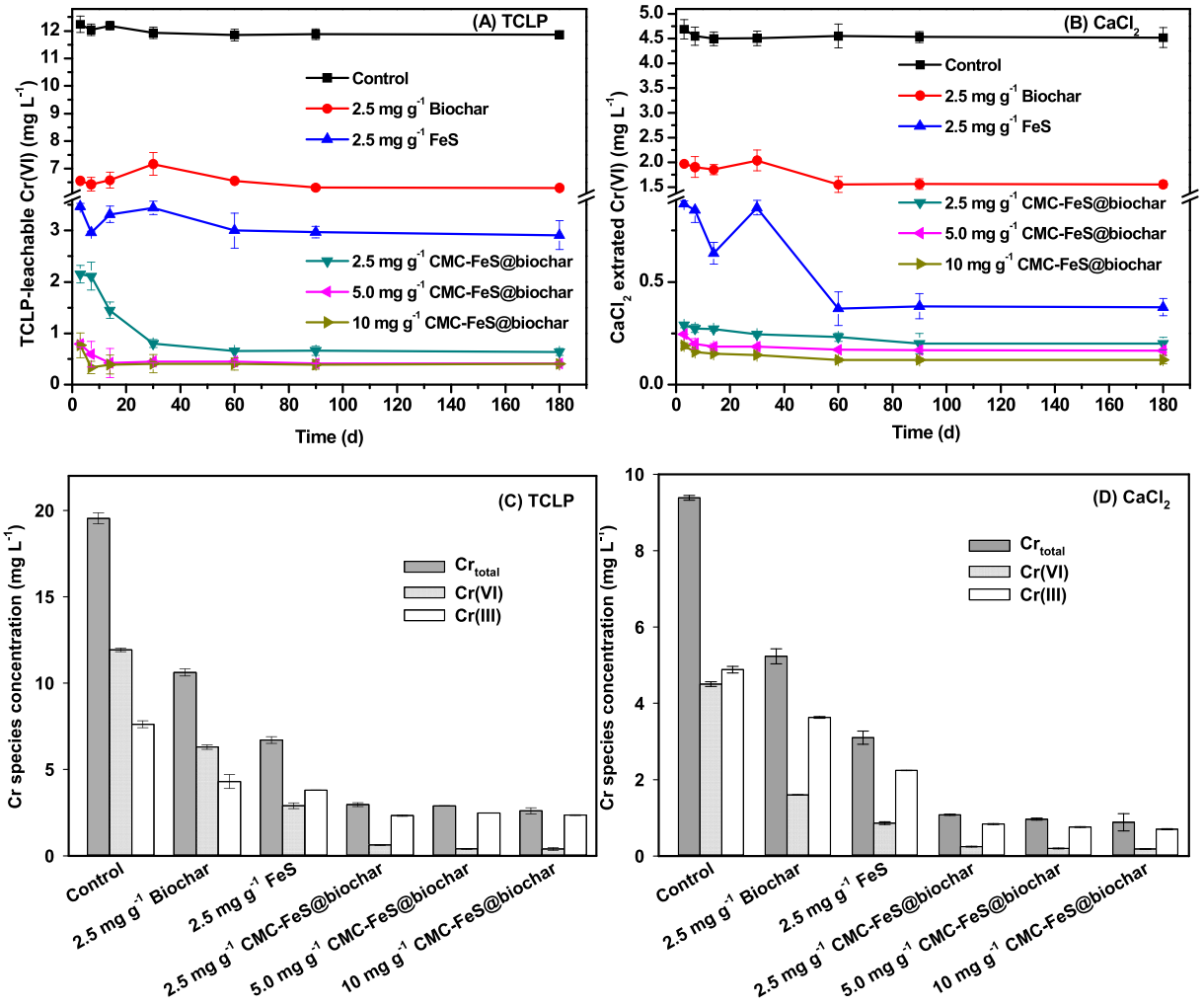

Fig. 3. Concentrations of Cr(VI) (A and B) and various Cr species (C and D) in the TCLP and $CaCl_2$ extracts from control and biochar-, FeS-, or CMC-FeS@biochar-treated soils. Experimental conditions: Initial soil Cr(VI) content = 210 ± 18 mg kg^{-1}, and moisture content = 20 ± 5%. Data plotted as mean of duplicates and error bars (calculated as standard deviation) indicate data reproducibility.

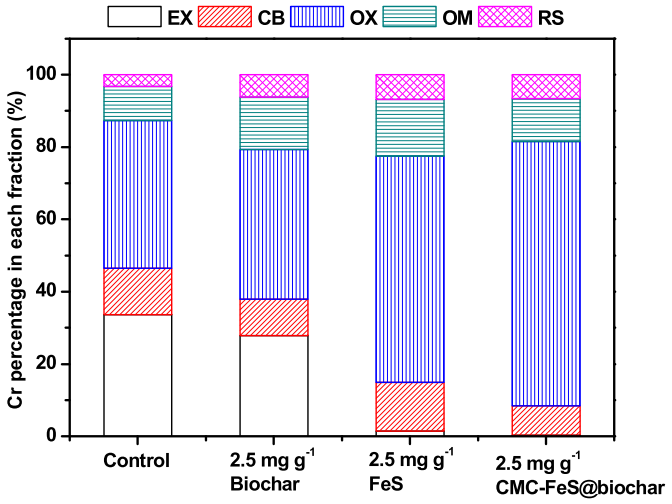

Fig. 4. Changes in Cr speciation in soil before and after 2.5 mg g^{-1} biochar-, 2.5 mg g^{-1} FeS-, or 2.5 mg g^{-1} CMC-FeS@biochar treatment. Experimental conditions: Initial soil Cr (VI) concentration = 210 ± 18 mg kg^{-1}, moisture content = 20 ± 5%, and incubation time = 180 d. Data plotted as mean of duplicates and error bars (calculated as standard deviation) indicate data reproducibility.

Upon 2.5 mg g^{-1} CMC-FeS@biochar treatment, C–C and C–O slightly decreased from 39.2% to 23.5%–31.6% and 21.3%, respectively (Fig. 5A), which might be due to the surface complexation between Cr(VI) and –COOH functional group (Zhang et al., 2017). In addition, C=O group increased from 10.6 to 17.4% probably due to the formation of C=O by the chemical redox reaction between Cr(VI) and C bond on the surface of CMC-FeS@biochar (Liu et al., 2012). For O 1s (Fig. 5B), a new peak corresponding to C=O appeared at 534.4 eV, and the percentages of C–O and –OH groups decreased from 61.7 to 59.9% and from 38.3 to 19.5%, respectively. These changes further proved the surface complexation between Cr(VI) and the functional groups (e.g., C–O and –OH) on CMC-FeS@biochar surface. Our previous results (Lyu et al., 2017) revealed that –OH, C=O, O=C–O, and C–O may play an important role in FeS particles soldering onto the surface of biochar via CMC. For CMC-FeS@biochar, the increased oxygen-containing functional groups, derived from biochar and CMC, may contribute to the immobilization of Cr(VI). The Fe 2p3/2 peak shifted slightly to 711.9, 713.8, and 724.6 eV, the percentage of Fe(II) decreased from 6.3 to 2.2% and Fe(III) in $Fe(OH)_3$ and/or Fe_2O_3 increased from 93.7 to 97.8% (Fig. 5C), which was due to the oxidation of Fe(II) by Cr(VI) during the treatment. Meanwhile, the peak of S (-II) disappeared (Fig. 5D). S(IV) and/or S(VI) shifted slightly to 168.7 and 171.8 eV,

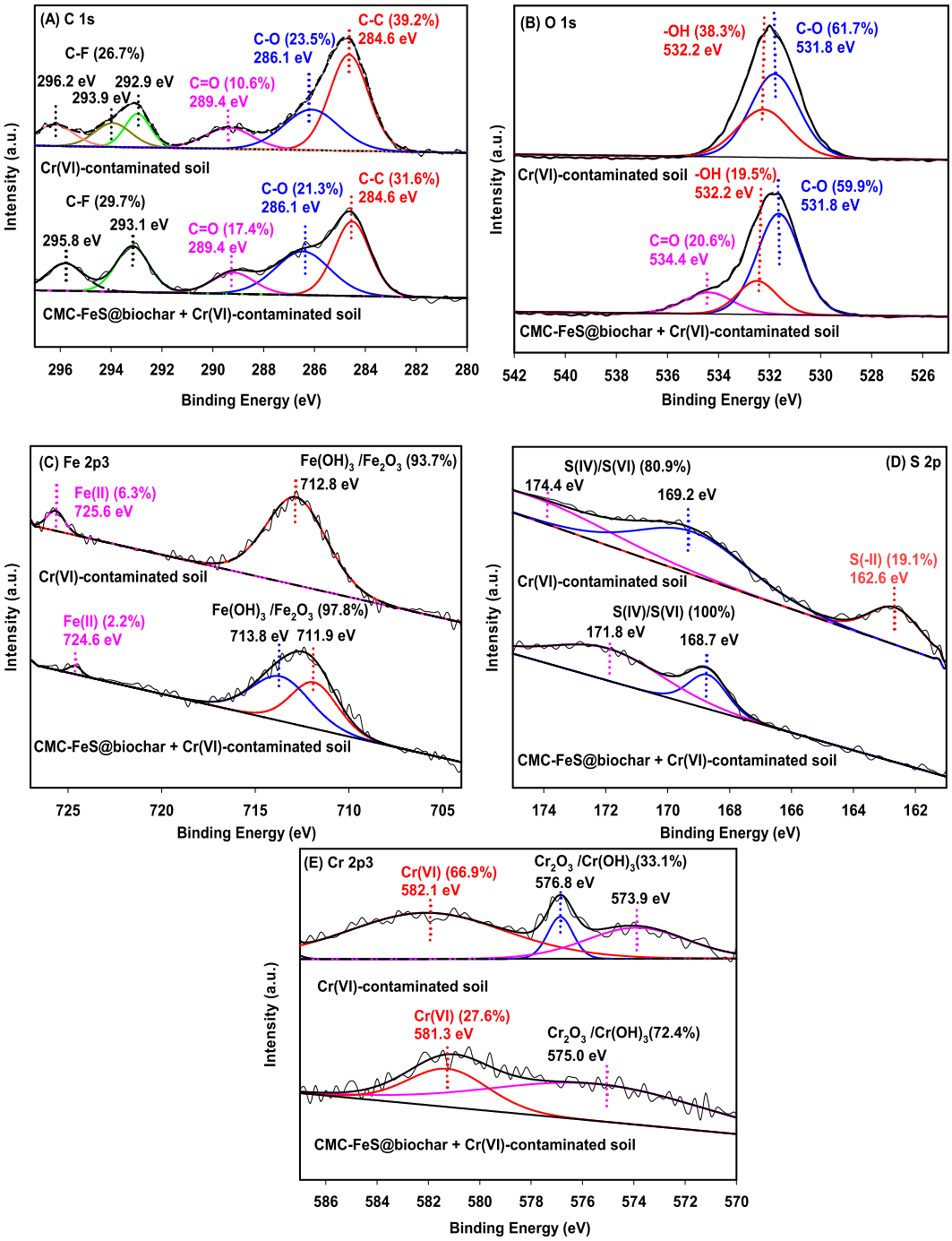

Fig. 5. XPS spectra of the soil before and after 2.5 mg g^{-1} CMC-FeS@biochar treatment: (A) C 1s, (B) O 1s, (C) Fe 2p3, (D) S 2p, and (E) Cr 2p3/2 spectra. CMC-FeS@biochar + Cr(VI)-contaminated soil preparation: CMC-FeS@biochar-to- Cr(VI)-contaminated soil mass ratio = 2.5 mg g^{-1}, initial soil Cr (VI) concentration = 210 ± 18 mg kg^{-1}, moisture content = 20 ± 5%, and incubation time = 180 d.

and increased from 80.9 to 100% after treatment, suggesting the oxidization of S (-II) by Cr(VI). Cr_2O_3 and/or $Cr(OH)_3$ peaks shifted to 575.0 eV and Cr(VI) shifted to 581.3 eV. The percentage of Cr_2O_3 and/or $Cr(OH)_3$ increased from 33.1 to 72.4% and that of Cr(VI) decreased from 66.9 to 27.6% (Fig. 5E), which was attributed to the redox reactions between CMC-FeS@biochar and Cr(VI).

The predominant Fe(II) and Cr(VI) species at pH > 7.5 (Table 1) were FeS and CrO_4^{2-} according to the Visual MINTEQ results (SI Fig. S1). Based on the SEP and XPS results, Cr(VI) immobilization by CMC-FeS@biochar mainly includes the following steps: (1) adsorption of Cr(VI) onto CMC-FeS@biochar surface via surface pores and oxygen-containing functional groups (C—C, C—O, C═O, and —OH), (2) reduction of Cr(VI) by Fe(II), S (-II) (Eqs. (1), (8)–(10)) (Lu et al., 2006), (3) reduction of Cr(VI) by the carbon surface (Eqs. (7) and (11)), and (4) precipitation of Cr_2O_3, $Cr(OH)_3$, Fe_2O_3, and $Fe(OH)_3$ (Lu et al., 2006).

$$FeS + H^+ \rightarrow Fe^{2+} + HS^- \quad (1)$$

$$3Fe^{2+} + HCrO_4^- + 7H^+ = 3Fe^{3+} + Cr^{3+} + 4H_2O \quad (2)$$

$$HS^- + 2HCrO_4^- + 7H^+ = SO_3^{2-} + 2Cr^{3+} + 5H_2 \quad (3)$$

$$8HS^- + 3HCrO_4^- + 29H^+ = 3SO_4^{2-} + 8Cr^{3+} + 20H_2O \quad (4)$$

$$HCrO_4^- + 7H^+ + 3e^- \leftrightarrow Cr^{3+} + 4H_2 \quad (5)$$

$$Surface - C - e^- \leftrightarrow Surface - CO_x \quad (6)$$

where Surface-C represents the C bond on the CMC-FeS@biochar surface, and Surface-COxH indicates the newly formed oxygen containing functional groups caused by the reduction of Cr(VI) and oxidation of surface C.

$$xCr^{3+} + (1-x)Fe^{3+} + 3H_2O = (Cr_xFe_{1-x})(OH)_3(s) + 3H^+ \quad (x<1) \quad (7)$$

$$3Fe^{2+} + CrO_4^{2-} + 4OH^- + 4H_2O = 3Fe(OH)_3(s) + Cr(OH)_3(s) \quad (8)$$

$$6Fe^{2+} + CrO_4^{2-} + 13OH^- = 3Fe_2O_3(s) + Cr(OH)_3(s) + 5H_2O \quad (9)$$

$$HS^- + 2Fe^{2+} + 2CrO_4^{2-} + 5OH^- = SO_4^{2-} + Cr_2O_3(s) + 2Fe(OH)_3(s) \quad (10)$$

$$CrO_4^{2-} + e^- \leftrightarrow Cr^{3+} + 6OH^- \quad (11)$$

3.4. Influence of CMC-FeS@biochar amendments on soil properties

Selected physical-chemical properties of soils are presented in Table 1. The Cr(VI)-contaminated soil (Cr(VI) content = 210 ± 18 mg kg^{-1}) had lower redox potential 374 ± 19 mV than the Cr(VI)-free soil (518 ± 30 mV), indicating the reduction of Cr(VI) by the reducing matters in soil (Zhang et al., 2016). No detectable TOC (<0.004 g kg^{-1}) was found in both Cr(VI)-free soil and Cr(VI)-contaminated soil. After Cr(VI) was spiked, pH of the soil decreased from 8.37 for Cr(VI)-free soil to 7.86 for Cr(VI)-contaminated soil.

Upon biochar, FeS, or CMC-FeS@biochar treatment, Cr_{total} content remained unchanged in all soils (from 305 ± 10 to 320 ± 24 mg kg^{-1}) while Cr(VI) contents were reduced to 128 ± 14, 69.4 ± 9.8, 12.9 ± 1.8, 9.0 ± 1.1, and 8.2 ± 0.9 by 2.5 mg g^{-1} biochar, 2.5 mg g^{-1} FeS, 2.5 mg g^{-1} CMC-FeS@biochar, 5.0 mg g^{-1} CMC-FeS@biochar, and 10 mg g^{-1} CMC-FeS@biochar, respectively. The redox potential of soils reduced from 374 ± 19 to 350 ± 13, 339 ± 15, 320 ± 17, 317 ± 12, and 300 ± 9 mV with the application of 2.5 mg g^{-1} biochar, 2.5 mg g^{-1} FeS, 2.5 mg g^{-1} CMC-FeS@biochar, 5.0 mg g^{-1} CMC-FeS@biochar, and 10 mg g^{-1} CMC-FeS@biochar, respectively. Furthermore, the addition of biochar, FeS, and CMC-FeS@biochar significantly increased soil TOC contents (Table 1). For instance, the TOC content increased from 13.1 ± 0.1 to 22.6 ± 0.9 g kg^{-1} as CMC-FeS@biochar dosage increased from 2.5 to 10 mg g^{-1}, indicating that the addition of biochar and CMC introduced carbon source into the soil. Moreover, the TOC content increased from <0.004 to 6.7 ± 1.3 g kg^{-1} when 2.5 mg g^{-1} FeS was applied, which suggested the increased activity of microbials ascribing to decreased toxicity of Cr(VI) (Spokas et al., 2009).

CO_2, CH_4, N_2O, and NH_3 concentrations before and after remediation were compared in Fig. 6. Upon 2.5 mg g^{-1} biochar, 2.5 mg g^{-1} FeS, or 2.5 mg g^{-1} CMC-FeS@biochar treatment, N_2O concentrations remained constant at 0.31–0.32 mg kg^{-1} (w w^{-1}); CO_2 significantly increased from 411 to 419, 554, and 558 mg kg^{-1}, respectively; CH_4 concentrations decreased from 1.99 to 1.91, 1.89, and 1.80 mg kg^{-1}, respectively; and NH_3 concentrations decreased from 0.19 to 0.14, 0.10, and 0.08 mg kg^{-1}, respectively. CO_2 represents the intensity of soil respiration of plant roots, the rhizosphere, microbes, and fauna (Sivakumar and Subbhuraam, 2005). The increased CO_2 concentration indicated the enhanced microbial activity, which was ascribed to (1) the decreased toxicity of Cr(VI) and (2) the carbon source produced by liable or reactive components adsorbed on the biochar and CMC (Sivakumar and Subbhuraam, 2005; Lyu et al., 2016b). CH_4 emissions from soil are the balance between methane-producing and methane-oxidizing bacteria (Seghers et al., 2003). The release of NH_3 and N_2O accounts for the strength of nitrification and denitrification (Yanai et al., 2007). The decreased CH_4 and NH_3 concentrations were ascribed to the increased activity of methane-oxidizing bacteria and ammonia oxidizing bacteria, respectively. In addition, the soil redox potential was reduced after treatment (Table 1), which was consistent with the findings by Yan et al. (2013), who reported that the increased activity of ammonia oxidizing bacteria would decrease the soil redox potential (Yan et al., 2013). Kludze et al. (1993) observed that a soil redox potential of < −150 mV was beneficial to CH_4 production, which further indicated the decrease of CH_4 concentration (Kludze et al., 1993; Ding and Cai, 2002).

3.5. Bioavailability to earthworm

After 15 d of exposure, all earthworms were alive in the Cr(VI)-free soil with low amount of Cr_{total} in earthworm body (0.07 mg g^{-1}) (Fig. 7A), which was ascribed to the low Cr concentration in the Cr(VI)-free soil (Cr_{total} = 31.1 ± 2.9 mg kg^{-1} and Cr(VI) < 0.16 mg kg^{-1}) (Table 1). No live earthworm was found in the control tests due to the high content of Cr (Cr_{total} = 320 ± 24 mg kg^{-1} and Cr(VI) = 210 ± 18 mg kg^{-1}) in Cr(VI)-contaminated soil (Table 1), resulting in a lethal amount of Cr_{total} accumulated in the earthworm body (0.23 mg g^{-1}). The addition of 2.5 mg g^{-1} biochar, 2.5 mg g^{-1} FeS, and 2.5 mg g^{-1} CMC-FeS@biochar significantly increased the earthworm survival rate (50% for 2.5 mg g^{-1} biochar, 75% for 2.5 mg g^{-1} FeS, and 90% for

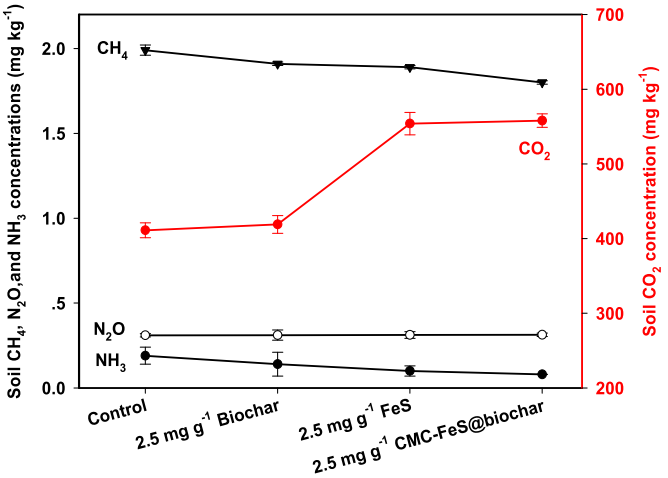

Fig. 6. Soil CH_4, N_2O, NH_3, and CO_2 concentrations before and after 2.5 mg g^{-1} biochar, 2.5 mg g^{-1} FeS, or 2.5 mg g^{-1} CMC-FeS@biochar treatment. Experimental conditions: Initial soil Cr (VI) concentration = 210 ± 18 mg kg^{-1}, moisture content = 20 ± 5%, and incubation time = 180 d. Data plotted as mean of duplicates and error bars (calculated as standard deviation) indicate data reproducibility.

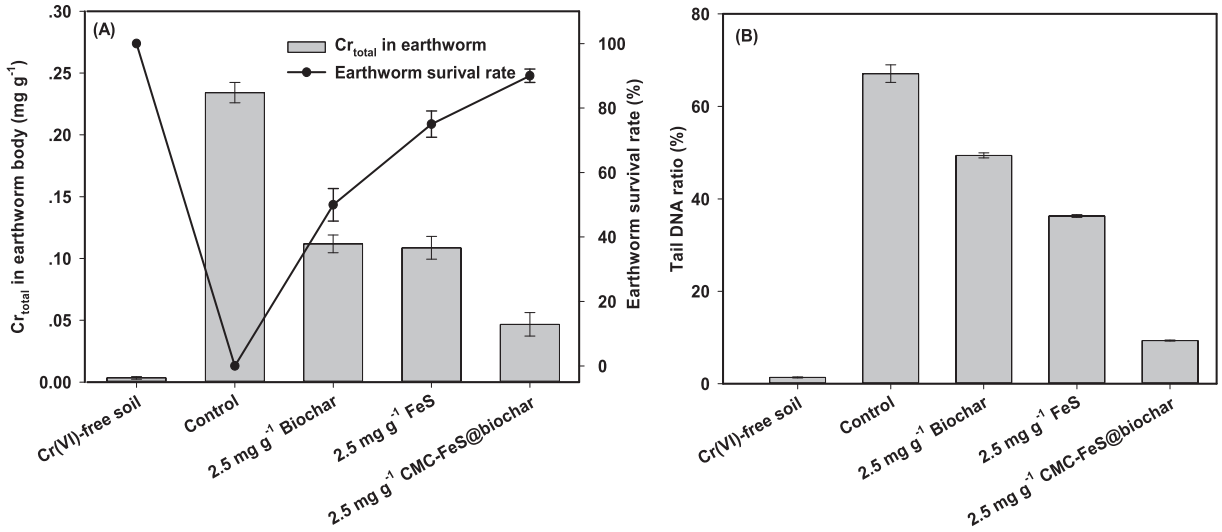

Fig. 7. (A) Uptake of Cr_{total} by earthworm and (B) earthworm DNA damage in Cr(VI)-free soil, control, and biochar-, FeS–, or CMC-FeS@biochar-treated soils.

2.5 mg g^{-1} CMC-FeS@biochar) and decreased the Cr_{total} content in earthworm body (0.11 mg g^{-1} for 2.5 mg g^{-1} biochar, 0.10 mg g^{-1} for 2.5 mg g^{-1} FeS, and 0.05 mg g^{-1} for 2.5 mg g^{-1} CMC-FeS@biochar). These trends were in good agreement with the results obtained from $CaCl_2$ extraction tests. After 180-d incubation experiment, the $CaCl_2$-extractable Cr(VI) concentration decreased by 65.5% for 2.5 mg g^{-1} biochar, 91.6% for 2.5 mg g^{-1} FeS, and 95.6% for 2.5 mg g^{-1} CMC-FeS@biochar. Tail DNA ratio, which is the ratio of intensity of comet tail to head, was used to evaluate the extent of DNA migration and the level of DNA damage in the comet assay (single-cell gel electrophoresis) (Fig. 7B). Higher earthworm DNA damage was observed for Cr(VI)-contaminated soil (67.1%) compared to Cr(VI)-free soil (1.36%). The application of biochar, FeS, and CMC-FeS@biochar resulted in less tail DNA (49.4% for biochar, 36.2% for FeS, and 9.31% for CMC-FeS@biochar). These results demonstrated that biochar, FeS, and CMC-FeS@biochar reduced the DNA damage induced by Cr(VI) in soils. CMC-FeS@biochar offered higher Cr(VI) immobilization ability than bare biochar and FeS, reducing the Cr(VI) bioavailability in soils.

3.6. Seed germination, early growth, and Cr bioaccumulation

The seedlings of wheat after 12 d in the presence of deionized water (blank), CMC-FeS@biochar, Cr(VI) solution, and Cr(VI)-laden CMC-FeS@biochar (i.e., CMC-FeS@biochar + Cr(VI) group) were compared (SI Fig. S2). Evidently, aqueous Cr(VI) showed a significantly inhibitory effects on wheat seedling growth (SI Fig. S2A). CMC-FeS@biochar and Cr(VI)-laden CMC-FeS@biochar had no significant toxic effect on the plants while the seedlings in dissolved Cr(VI) solution were small and unhealthy. The average germination rate of wheat after 2 d followed the order of blank (90.0%) > CMC-FeS@biochar (87.5%) = CMC-FeS@biochar + Cr(VI) (87.5%) > Cr(VI) (70.0%) (SI Fig. S2B). The following orders of average germinal lengths of wheat on 12th day holds: CMC-FeS@biochar (15.7 cm) > CMC-FeS@biochar + Cr(VI) (15.4 cm) > blank (15.2 cm) > Cr(VI) (8.0 cm) (SI Fig. S2C). Generally, Cr(VI) greatly inhibited the germination rate and germinal length of wheat, and the addition of CMC-FeS@biochar transformed the Cr(VI) to Cr(III), therefore reduced the biological toxicity of Cr(VI) (Wang et al., 2014; Su et al., 2016). Based on the *t*-tests, the differences between germination rates and seedling lengths of wheat with or without the addition of CMC-FeS@biochar are statistically significant with a *p* value of 0.002 and 0.001, respectively, at the 0.05 level of significance. The Cr_{total} contents in the dried wheat seeding were determined and the result is shown in SI Fig. S2D. No detectable Cr_{total} (<4.3 μg L^{-1}) was observed in the blank tests and the CMC-FeS@biochar group. High levels of Cr_{total} were found in the seedlings of the dissolved Cr(VI) group (1.19 mg g^{-1}), while the Cr_{total} content in the wheat was sharply decreased to 0.36 mg g^{-1} (a 69.7% decrease) when Cr(VI) was sorbed by CMC-FeS@biochar. The results indicated that the CMC-FeS@biochar significantly decreased the Cr_{total} uptake of wheat seeding, and thus, reducing the ecological risks of Cr(VI) to plants.

4. Conclusion

The CMC-FeS@biochar composite was designed as a highly promising material for *in situ* remediation of Cr(VI)-contaminated soil. CMC-FeS@biochar showed higher immobilization capacity of Cr(VI) than respective plain biochar and bare FeS, with significant reduction in Cr(VI) concentrations in TCLP and $CaCl_2$ extracts. The Cr(VI) immobilization process was a hybrid sorption-reduction/precipitation process. CMC-FeS@biochar promoted the conversion of more accessible Cr (EX and CB) into the less accessible forms (OX, OM, and RS), thus reduced bioavailability to wheat and earthworms. The addition of CMC-FeS@biochar increased soil organic matter and enhanced microbial activity, and can be used as an effective way of improving soil properties besides remediating Cr(VI)-contaminated soils. Thus, CMC-FeS@biochar composite, combining the advantages of biochar, CMC, and FeS, may bring multiple benefits, namely, reuse of solid waste, soil improvement, and remediation of contaminated soils.

Acknowledgements

The research was supported by Tianjin Research Program of Application Foundation and Advanced Technology (15JCYBJC53800), National Natural Science Foundation of China (41503085, 41473070), Scientific Research Foundation for Returned Overseas Chinese Scholars, Ministry of Education of China ([2015] 1098), The National Water Pollution Control and Treatment Science and Technology Major Project (2015ZX07203-011-06), and 863 achievement transformation program in Tianjin (No. 14RCHZSF00144).

Appendix A. Supplementary data

Supplementary data related to this article can be found at https://doi.org/10.1016/j.chemosphere.2017.11.182.

References

Ahmad, M., Rajapaksha, A.U., Lim, J.E., Zhang, M., Bolan, N., Mohan, D., Vithanage, M., Lee, S.S., Ok, Y.S., 2014. Biochar as a sorbent for contaminant management in soil and water: a review. Chemosphere 99, 19–33.

Ajmal, M., Nomani, A.A., Ahmad, A., 1984. Acute toxicity of chrome electroplating wastes to microorganisms: adsorption of chromate and chromium (VI) on a mixture of clay and sand. Water Air Soil Pollut. 23, 119–127.

Briggs, D., Seah, M.P., 1993. Practical Surface Analysis, second ed. John Willey Sons, New York.

Cao, X., Ma, L., Liang, Y., Gao, B., Harris, W., 2011. Simultaneous immobilization of lead and atrazine in contaminated soils using dairy-manure biochar. Environ. Sci. Technol. 45, 4884–4889.

Choppala, G., Bolan, N., Kunhikrishnan, A., Skinner, W., Seshadri, B., 2015. Concomitant reduction and immobilization of chromium in relation to its bioavailability in soils. Environ. Sci. Pollut. Res. Int. 22, 8969–8978.

Choppala, G.K., Bolan, N.S., Megharaj, M., Chen, Z., Naidu, R., 2012. The influence of biochar and black carbon on reduction and bioavailability of chromate in soils. J. Environ. Qual. 41, 1175–1184.

Ding, W., Cai, Z., 2002. Effects of soil organic matter and exogenous organic materials on methane production in and emission from wetlands. Acta Ecol. Sin. 22, 1672–1679 (in Chinese).

Dotaniya, M.L., Meena, V.D., Das, H., 2014. Chromium toxicity on seed germination, root elongation and coleoptile growth of pigeon pea (cajanus cajan). Legume Res. 37, 227–229.

EPD, MLR, 2014. The Environmental Protection Department and the Ministry of Land and Resources Issued the National Soil Pollution Condition Investigation Communique. http://www.mlr.gov.cn/xwdt/jrxw/201404/t20140417_21312998.htm.

Faisal, M., Hasnain, S., 2005. Bacterial Cr (VI) reduction concurrently improves sunflower (Helianthus annuus L.) growth. Biotechnol. Lett. 27, 943–947.

Fang, S.E., Tsang, D.C.W., Zhou, F.S., Zhang, W.H., Qiu, R.L., 2016. Stabilization of cationic and anionic metal species in contaminated soils using sludge-derived biochar. Chemosphere 149, 263–271.

Gong, Y., Liu, Y., Xiong, Z., Zhao, D., 2014. Immobilization of mercury by carboxymethyl cellulose stabilized iron sulfide nanoparticles: reaction mechanisms and effects of stabilizer and water chemistry. Environ. Sci. Technol. 48, 3986–3994.

Henderson, A.D., Demond, A.H., 2011. Impact of solids formation and gas production on the permeability of ZVI PRBs. J. Environ. Eng. 137, 689–696.

Hu, X., Zhou, M., Zhou, Q., 2015. Ambient water and visible-light irradiation drive changes in graphene morphology, structure, surface chemistry, aggregation, and toxicity. Environ. Sci. Technol. 49, 3410–3418.

Husson, O., 2013. Redox potential (Eh) and pH as drivers of soil/plant/microorganism systems: a transdisciplinary overview pointing to integrative opportunities for agronomy. Plant Soil 362, 389–417.

Kludze, H., DeLaune, R., Patrick, W., 1993. Aerenchyma formation and methane and oxygen exchange in rice. Soil Sci. Soc. Am. J. 57, 386–391.

Koenig, J.C., Boparai, H.K., Lee, M.J., O'Carroll, D.M., Barnes, R.J., Manefield, M.J., 2016. Particles and enzymes: combining nanoscale zero valent iron and organochlorine respiring bacteria for the detoxification of chloroethane mixtures. J. Hazard. Mater 308, 106–112.

Liu, W., Zhang, J., Zhang, C., Ren, L., 2012. Preparation and evaluation of activated carbon-based iron-containing adsorbents for enhanced Cr(VI) removal: mechanism study. Chem. Eng. J. 189–190, 295–302.

Liu, W., Zhang, J., Zhang, C., Wang, Y., Li, Y., 2010a. Adsorptive removal of Cr (VI) by Fe-modified activated carbon prepared from Trapa natans husk. Chem. Eng. J. 162, 677–684.

Liu, Y., Zhou, Q., Xie, X., Lin, D., Dong, L., 2010b. Oxidative stress and DNA damage in the earthworm Eisenia fetida induced by toluene, ethylbenzene and xylene. Ecotoxicology 19, 1551–1559.

Lu, A.H., Zhong, S.J., Chen, J., Shi, J.X., Tang, J.L., Lu, X.Y., 2006. Removal of Cr(VI) and Cr(III) from aqueous solutions and industrial wastewaters by natural clinopyrrhotite. Environ. Sci. Technol. 40, 3064–3069.

Lyu, H., Gong, Y., Tang, J., Huang, Y., Wang, Q., 2016a. Immobilization of heavy metals in electroplating sludge by biochar and iron sulfide. Environ. Sci. Pollut. Res. Int. 1–17.

Lyu, H., He, Y., Tang, J., Hecker, M., Liu, Q., Jones, P.D., Codling, G., Giesy, J.P., 2016b. Effect of pyrolysis temperature on potential toxicity of biochar if applied to the environment. Environ. Pollut. 218, 1–7.

Lyu, H., Tang, J., Huang, Y., Gai, L., Zeng, E.Y., Liber, K., Gong, Y., 2017. Removal of hexavalent chromium from aqueous solutions by a novel biochar supported nanoscale iron sulfide composite. Chem. Eng. J. 322, 516–524.

Mahdieh, K., Shahin, O., Nosratollah, N., Alireza, K., 2016. Treatment of Cr(VI)-spiked soils using sulfur-based amendments. Arch. Agron. Soil Sci. 62, 1474–1485.

MEPPRC, 2008. Standard for Pollution Control on the Landfill Site for the Municipal Solid Waste. PRC (in Chinese).

Petersen, E.J., Pinto, R.A., Landrum, P.F., Weber Jr., W.J., 2009. Influence of carbon nanotubes on pyrene bioaccumulation from contaminated soils by earthworms. Environ. Sci. Technol. 43, 4178–4181.

Seghers, D., Verthé, K., Reheul, D., Bulcke, R., Siciliano, S.D., Verstraete, W., Top, E.M., 2003. Effect of long-term herbicide applications on the bacterial community structure and function in an agricultural soil. FEMS Microbiol. Ecol. 46, 139–146.

Sivakumar, S., Subbhuraam, C.V., 2005. Toxicity of chromium(III) and chromium(VI) to the earthworm Eisenia fetida. Ecotoxicol. Environ. Saf. 62, 93–98.

Spokas, K., Koskinen, W., Baker, J., Reicosky, D., 2009. Impacts of woodchip biochar additions on greenhouse gas production and sorption/degradation of two herbicides in a Minnesota soil. Chemosphere 77, 574–581.

Su, H., Fang, Z., Tsang, P.E., Fang, J., Zhao, D., 2016. Stabilisation of nanoscale zerovalent iron with biochar for enhanced transport and in-situ remediation of hexavalent chromium in soil. Environ. Pollut. 214, 94–100.

Sun, Y.N., Gao, B., Yao, Y., Fang, J.N., Zhang, M., Zhou, Y.M., Chen, H., Yang, L.Y., 2014. Effects of feedstock type, production method, and pyrolysis temperature on biochar and hydrochar properties. Chem. Eng. J. 240, 574–578.

Tessier, A., Campbell, P.G., Bisson, M., 1979. Sequential extraction procedure for the speciation of particulate trace metals. Anal. Chem. 51, 844–851.

Wagner, C.D., 1978. X-ray photoelectron spectroscopy with x-ray photons of higher energy. J. Vac. Sci. Technol. 15, 518–523.

Wang, Y., Fang, Z., Kang, Y., Tsang, E.P., 2014. Immobilization and phytotoxicity of chromium in contaminated soil remediated by CMC-stabilized nZVI. J. Hazard. Mater 275, 230–237.

Wu, L., Lyu, H., Su, C., Zeng, D., Mo, X., 2014. Remediation of heavy metals contaminated soil by washing with environmentally friendly washing liquids. J. Environ. Eng. 8, 4486–4491 (in Chinese).

Yan, J., Han, L., Gao, W., Xue, S., Chen, M., 2014. Biochar supported nanoscale zerovalent iron composite used as persulfate activator for removing trichloroethylene. Bioresour. Technol. 175C, 269–274.

Yan, Y., Wang, D., Zheng, J., 2013. Advances in effects of biochar on the soil N2O and CH4 emissions. Agric. Sci. Bull. 29, 140–146 (in Chinese).

Yanai, Y., Toyota, K., Okazaki, M., 2007. Effects of charcoal addition on N2O emissions from soil resulting from rewetting air-dried soil in short-term laboratory experiments. Soil Sci. Plant Nutr. 53, 181–188.

Yang, R., Wang, Y., Li, M., Hong, Y., 2014. A new carbon/ferrous sulfide/iron composite prepared by an in situ carbonization reduction method from hemp (cannabis sativaL.) stems and its Cr(VI) removal ability. ACS Chem. Eng. 2, 1270–1279.

Zhang, H., Tang, J., Wang, L., Liu, J., Gurav, R.G., Sun, K., 2016. A novel bioremediation strategy for petroleum hydrocarbon pollutants using salt tolerant Corynebacterium variable HRJ4 and biochar. J. Environ. Sci. (China) 47, 7–13.

Zhang, J., Chen, S., Zhang, H., Wang, X., 2017. Removal behaviors and mechanisms of hexavalent chromium from aqueous solution by cephalosporin residue and derived chars. Bioresour. Technol. 238, 484–491.

Zhou, J.-H., Sui, Z.-J., Zhu, J., Li, P., Chen, D., Dai, Y.-C., Yuan, W.-K., 2007. Characterization of surface oxygen complexes on carbon nanofibers by TPD, XPS and FT-IR. Carbon 45, 785–796.

Zhou, Y., Gao, B., Zimmerman, A.R., Fang, J., Sun, Y., Cao, X., 2013. Sorption of heavy metals on chitosan-modified biochars and its biological effects. Chem. Eng. J. 231, 512–518.